

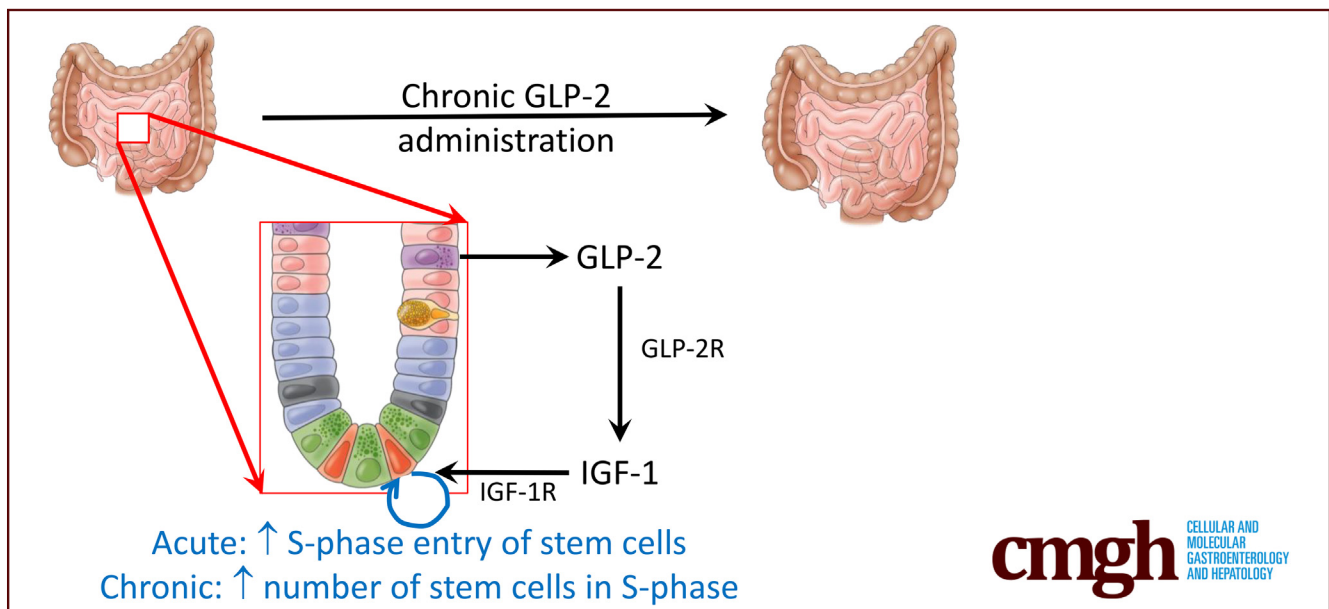
ORIGINAL RESEARCH

Glucagon-Like Peptide-2 Stimulates S-Phase Entry of Intestinal Lgr5 + Stem Cells



Maegan E. Chen,¹ Setareh Malekian Naeini,¹ Arjuna Srikrishnaraj,¹ Daniel J. Drucker,² Zivit Fesler,¹ and Patricia L. Brubaker^{1,2}

¹Department of Physiology, ²Department of Medicine, University of Toronto, Toronto, Ontario, Canada



SUMMARY

Glucagon-like peptide-2, a hormone that enhances bowel growth and function in patients with short-bowel syndrome, is identified as a novel factor that acutely stimulates S-phase entry of the intestinal leucine-rich repeat-containing G-protein-coupled receptor 5+ stem cell and chronically increases intestinal leucine-rich repeat-containing G-protein-coupled receptor 5+ stem cell numbers.

BACKGROUND & AIMS: Leucine-rich repeat-containing G-protein-coupled receptor-5 (*Lgr5*)+/olfactomedin-4 (*Olfm4*) + intestinal stem cells (ISCs) in the crypt base are crucial for homeostatic maintenance of the epithelium. The gut hormone, glucagon-like peptide-2¹⁻³³ (GLP-2), stimulates intestinal proliferation and growth; however, the actions of GLP-2 on the *Lgr5* + ISCs remain unclear. The aim of this study was to determine whether and how GLP-2 regulates *Lgr5* + ISC cell-cycle dynamics and numbers.

METHODS: *Lgr5*-Enhanced green-fluorescent protein - internal ribosome entry site - Cre recombinase - estrogen receptor T2 (eGFP-IRES-creERT2) mice were acutely administered human Glycine² (Gly2)-GLP-2, or the GLP-2-receptor antagonist, GLP-2³⁻³³.

Intestinal epithelial insulin-like growth factor-1-receptor knockout and control mice were treated chronically with human Gly2 (hGly2)-GLP-2. Cell-cycle parameters were determined by 5-Ethynyl-2'-deoxyuridine (EdU), bromodeoxyuridine, antibody #Ki67, and phospho-histone 3 labeling and cell-cycle gene expression.

RESULTS: Acute hGly2-GLP-2 treatment increased the proportion of eGFP+EdU+/OLFM4+EdU+ cells by 11% to 22% ($P < .05$), without affecting other cell-cycle markers. hGly2-GLP-2 treatment also increased the ratio of eGFP+ cells in early to late S-phase by 97% ($P < .001$), and increased the proportion of eGFP+ cells entering S-phase by 218% ($P < .001$). hGly2-GLP-2 treatment induced jejunal expression of genes involved in cell-cycle regulation ($P < .05$), and increased expression of *Mcm3* in the *Lgr5*-expressing cells by 122% ($P < .05$). Conversely, GLP-2³⁻³³ reduced the proportion of eGFP+EdU+ cells by 27% ($P < .05$), as well as the expression of jejunal cell-cycle genes ($P < .05$). Finally, chronic hGly2-GLP-2 treatment increased the number of OLFM4+ cells/crypt ($P < .05$), in an intestinal epithelial insulin-like growth factor-1-receptor-dependent manner.

CONCLUSIONS: These findings expand the actions of GLP-2 to encompass acute stimulation of *Lgr5* + ISC S-phase entry through the GLP-2R, and chronic induction of *Lgr5* + ISC expansion through downstream intestinal insulin-like growth factor-1

signaling. (*Cell Mol Gastroenterol Hepatol* 2022;13:1829–1842; <https://doi.org/10.1016/j.jcmgh.2022.02.011>)

Keywords: Cell Cycle; GLP-2; Intestine; Lgr5; Olfm4; Proliferation; S-Phase.

Two distinct crypt cell populations proliferate within the intestinal epithelium to maintain homeostasis: the intestinal stem cells (ISCs; also known as the crypt base columnar cells), which reside between the Paneth cells in positions 1–3, and their daughter cells in the transit-amplifying zone (TA) that also differentiate to generate the mature epithelium.^{1–4} Several molecular markers have been established to identify the ISCs, most notably, leucine-rich repeat-containing G-protein-coupled receptor 5 (Lgr5) and olfactomedin-4 (Olfm4).^{2,3,5} ISCs have a well-defined cell-cycle length of 24 hours, which is mediated through a novel growth 1 (G1) cell-cycle phase.^{2,6} Hence, approximately 60%–70% of the Lgr5+ ISCs reside in a prolonged G1 phase, awaiting licensing to proceed into the synthesis (S)-phase.⁶ ISC licensing to S-phase is mediated, in part, through minichromosome maintenance (MCM)2–7 complexes loading onto the DNA origins of replication.^{6,7} In addition, cyclin D1 is up-regulated to mediate cell-cycle passage through the G1/S-phase checkpoint.¹ This extended unlicensed G1 phase allows the ISCs to respond in a temporal manner to surrounding niche signals, including R-spondin, Notch, bone morphogenic protein, Wingless-related integration site (Wnt), insulin-like growth factor (IGF)-1, and Epidermal growth factor family of receptors (ErbB) ligands.^{4,8–11}

The intestinotrophic hormone, glucagon-like peptide-2 (GLP-2), is secreted by the enteroendocrine L cell and enables homeostatic maintenance of the intestinal epithelium.^{12–15} Upon binding to its receptor (GLP-2R), GLP-2 initiates signals promoting proliferation of the intestinal crypt cells, resulting in increased intestinal growth and improved intestinal digestive, absorptive, and barrier functions.^{16,17} Interestingly, the GLP-2R is not expressed in the gut epithelial cells but is localized to cells within the lamina propria as well as in scattered neurons of the enteric nervous system.¹⁸ Hence, the intestinotrophic actions of GLP-2 are exerted indirectly through downstream signaling mediators arising from the niche, including IGF-1 and ErbB family ligands.^{19–22} Because of its intestinal-specific actions, a degradation-resistant GLP-2R agonist, teduglutide (human [h]Glycine²[Gly2]-GLP-2), has been developed for use in patients with short-bowel syndrome, reducing the need for parenteral nutrition while increasing both the size and absorptive function of the intestinal epithelium.^{23–26}


Analyses of proliferative markers, including bromodeoxyuridine (BrdU) or 5-Ethynyl-2'-deoxyuridine (EdU) incorporation for S-phase and/or the general G1/S/G2/M-phase marker antibody #Ki-67 (Ki67), have shown that GLP-2 stimulates proliferation of the transit-amplifying cells in a manner that requires a full complement of B-cell lymphoma Moloney murine leukemia virus insertion region-1 homolog, a polycomb-repressive complex chromatin-remodeling protein that promotes stem cell proliferation and self-renewal.^{19,20,27,28} GLP-2 also stimulates expansion

of the columnar cell progenitor population as well as crypt cell mitotic index and crypt fission in human beings and rodent models.^{24,29,30} Although previous studies have examined the incorporation of S-phase markers into the intestinal stem cell zone in response to GLP-2 administration, these studies have been limited by the use of positional cell-counting analyses that did not distinguish between ISCs and the nonproliferative Paneth cells in the crypt base, which, thereby, diluted any possible signal from the proliferating ISCs at each cell position.^{19,20,27,28} It therefore remains unknown as to whether the ISCs proliferate in response to GLP-2. Furthermore, single-cell sequencing has shown that GLP-2R is not expressed by the ISCs, although they do express the IGF-1 and ErbB receptors,^{31,32} with both signaling pathways stimulating ISC proliferation and population expansion.^{8,33,34} In addition, GLP-2 treatment stimulates crypt cell Wnt signaling through the insulin-like growth factor-1 receptor (IGF-1R), inducing nuclear translocation of β -catenin in the crypt cells, as well as inducing expression of messenger RNA transcripts for cellular myelocytomatosis oncogene in the mucosa,³⁵ although, again, these markers of proliferation were not localized to the ISCs themselves. The overall aim of the present study, therefore, was to determine whether GLP-2 induces proliferation of the Lgr5+/Olfm4+ ISCs and, if so, to examine the underlying mechanism(s) of action of this intestinotrophic hormone.

Results

To determine the role of GLP-2 in ISC proliferation and cell-cycle progression, Lgr5-Enhanced green-fluorescent protein - internal ribosome entry site - Cre recombinase - estrogen receptor T2 (eGFP-IRES-creERT2) mice were treated with hGly2-GLP-2 or vehicle at 6 and 3 hours before being killed; at 1 hour before being killed, EdU was administered to label cells in S-phase³⁶ (Figure 1A). As expected, eGFP+ cells were restricted to the crypt base, with 27% showing colocalization with EdU, indicative of S-phase (Figure 1B and C). Acute hGly2-GLP-2 treatment increased the proportion of eGFP+ cells in S-phase by 11% ($P < .05$). To confirm these findings, immunostaining for the endogenous ISC marker, OLFM4, was performed next. OLFM4+ cells also were observed at the crypt base, of which 39%

Abbreviations used in this paper: BrdU, bromodeoxyuridine; creERT2, Cre recombinase - estrogen receptor T2; EdU, 5-Ethynyl-2'-deoxyuridine; EGF, epidermal growth factor; eGFP, Enhanced green-fluorescent protein; ErbB, Epidermal growth factor family of receptors; GLP-2, glucagon-like peptide-2; GLP-2R, glucagon-like peptide-2 receptor; Gly2, Glycine²; G1, growth 1; hGly2, human Gly2; IE, Intestinal epithelial; IGF, insulin-like growth factor; IGF-1R, insulin-like growth factor-1 receptor; IRES, internal ribosome entry site; ISC, intestinal stem cells; Ki67, antibody #Ki-67; KO, knockout; Lgr5, leucine-rich repeat-containing G-protein-coupled receptor 5; MCM, minichromosome maintenance; Olfm4, olfactomedin-4; pH3, phospho-histone 3; S-phase, synthesis phase; Wnt, Wingless-related integration site.

 Most current article

© 2022 The Authors. Published by Elsevier Inc. on behalf of the AGA Institute. This is an open access article under the CC BY-NC-ND license (<http://creativecommons.org/licenses/by-nc-nd/4.0/>).

2352-345X

<https://doi.org/10.1016/j.jcmgh.2022.02.011>

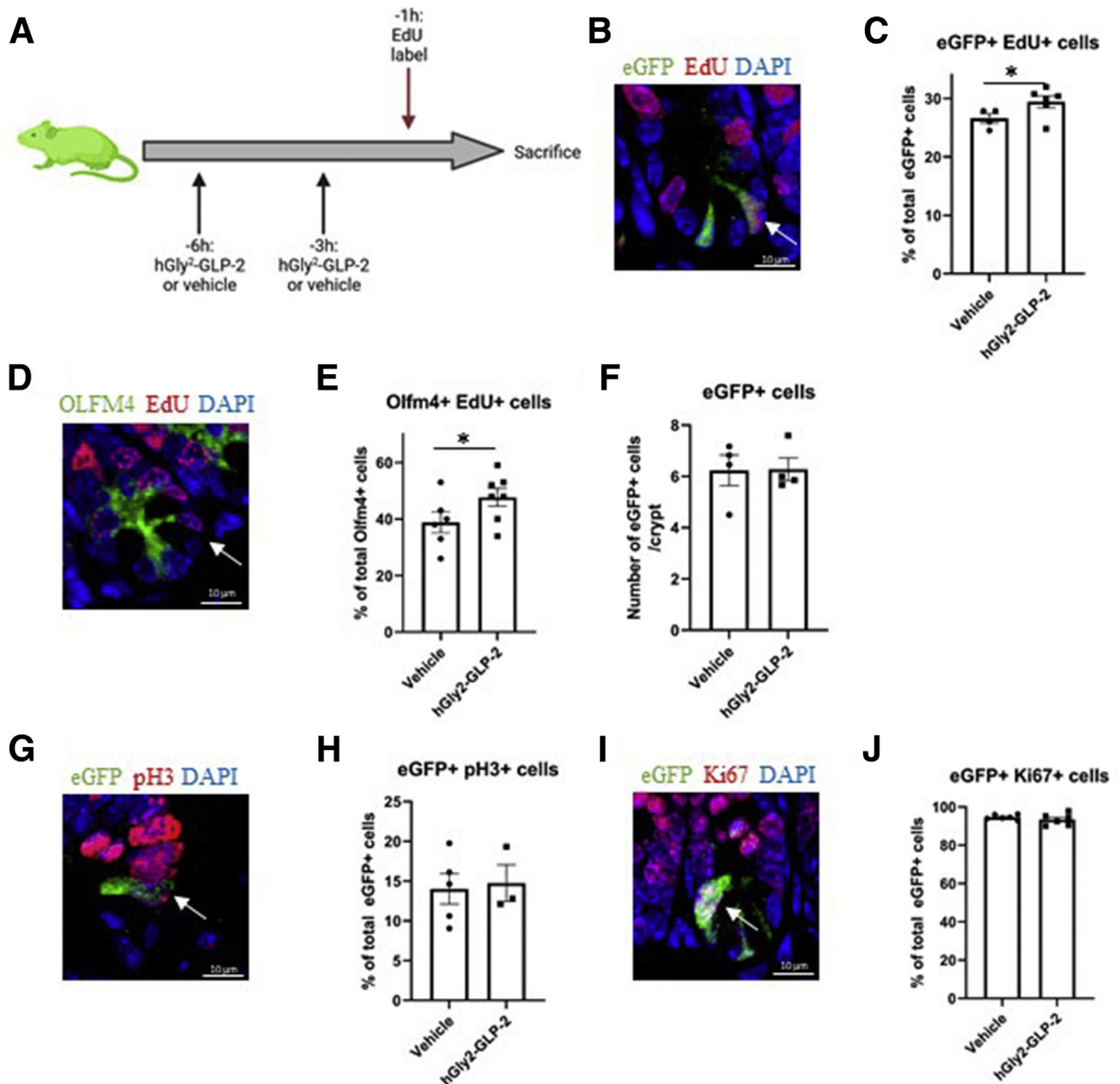


Figure 1. Acute hGly2-GLP-2 treatment increases the proportion of jejunal Lgr5+ /Olfm4+ ISCs in S-phase. (A) Acute hGly2-GLP-2 treatment protocol; the green mouse indicates use of Lgr5-eGFP-IRES-creERT2 animals (created using Biorender.com). (B) Representative image of eGFP+EdU+ ISCs (white arrow) and the (C) percentage of total eGFP+ ISCs that incorporated EdU. (D) Representative image of OLFM4+EdU+ ISC (white arrow) and the (E) percentage of total OLFM4+ ISCs that incorporated EdU. (F) Total number of eGFP+ ISCs per crypt. (G) Representative image of eGFP+ p3+ ISC (white arrow) and the (H) percentage of total eGFP+ cells that were also p3+. (I) Representative image of ISCs (white arrow) and the (J) percentage of total eGFP+ cells that also were Ki67+. (C, E, F, H, and J) N = 4–7. *P < .05. DAPI, 4',6-diamidino-2-phenylindole.

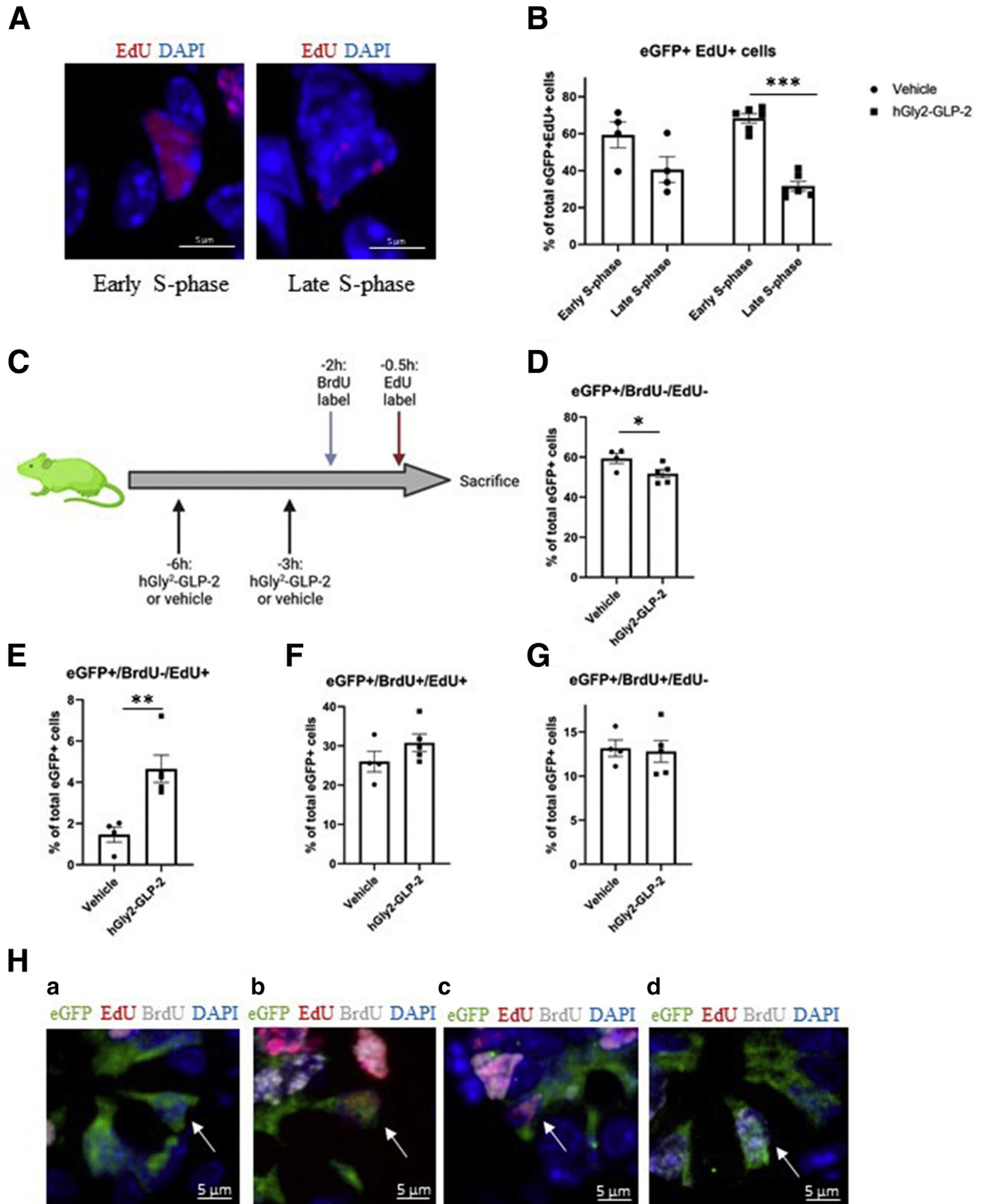
colocalized with EdU (Figure 1D and E). Consistent with the findings described for the eGFP+ cells, hGly2-GLP-2 increased the proportion of OLFM4+EdU+ cells by 22% (P < .05). The increases in the proportion of ISCs in S-phase occurred without a change in the total number of eGFP+ cells per crypt (Figure 1F). In contrast to the findings with EdU, 14% of the eGFP+ cells colocalized with the M-phase marker phospho-histone 3 (pH3),³⁷ and this proportion did not

change with acute hGly2-GLP-2 treatment (Figure 1G and H). Furthermore, 95% of the eGFP+ cells colocalized with the G1/S/G2/M-phase cell-cycle marker Ki67,³⁸ and this proportion also was not different with hGly2-GLP-2 administration (Figure 1I and J). These findings are consistent with S-phase induction of the ISCs by acute administration of GLP-2.

To identify the early vs late stages of S-phase, eGFP+EdU+ cells were examined for full nuclear EdU

staining (early S-phase) or punctate nuclear EdU staining (Figure 2A), as reported.^{6,39} The proportion of eGFP+EdU+ cells in early vs late S-phase was not different in vehicle-

treated animals (Figure 2B). However, hGly2-GLP-2 acutely increased the proportion of eGFP+ cells in early vs late S-phase (67% vs 33%; $P < .001$), resulting in an overall



97% ($P < .001$) increase in the ratio of cells in early to late S-phase compared with vehicle-treated mice. BrdU and EdU then were administered at 2 and 0.5 hours before being killed, respectively, to generate 4 different cell types representing the 1.5-hour temporal gap between the 2 labels: cells not in S-phase (BrdU-EdU-), cells entering S-phase (BrdU-EdU+), cells that remained in S-phase (BrdU+EdU+), and cells that exited S-phase (BrdU+EdU-) (Figures 2C–H). Consistent with the findings in Figure 1, hGly2–GLP-2 administration decreased the proportion of eGFP+ cells that were not in S-phase by 15% compared with vehicle ($P < .05$) (Figure 2D and Ha). However, concomitantly, hGly2–GLP-2 increased the proportion of eGFP+ cells entering S-phase by 218% ($P < .001$) (Figure 2E and Hb), although did not alter the proportion of cells that remained in S-phase or exited S-phase (Figure 2F, G, and Hc and d). Together, these results show that acute GLP-2 treatment increases the proportion of ISCs in S-phase by inducing entry into early S-phase.

To identify potential targets that might mediate the proliferative actions of GLP-2 in the intestine, CD1 mice were treated with hGly2–GLP-2 or vehicle for 1–25 hours and the transcriptomes of whole-thickness jejunal and colonic sections were analyzed by microarray (Supplementary Data Set 1). Interestingly, expression of *Mcm3* was found to be increased in both the jejunum and colon at $t = 4$ hours, while *s100a6* was up-regulated at 4 hours in the jejunum only. Reverse-transcription quantitative polymerase chain reaction analysis of jejunal mucosa further showed that hGly2–GLP-2 increased the expression of several MCM family members, including *Mcm2*, *Mcm3*, *Mcm5*, and *Mcm7* ($P < .05$), but not *Mcm4* or *Mcm6* (Figure 3). Furthermore, hGly2–GLP-2 administration also increased the expression of *Cdk2*, *Ccnd1*, and *s100a6* ($P < .05$), all of which play roles in the G1/S-phase transition.^{7,40,41} Finally, to determine whether changes in mucosal cell-cycle gene expression occurred at the level of the ISC, RNAscope analysis was performed to examine colocalization of transcripts for *Mcm2*, *Mcm3*, *Cdk2*, and *Ccnd1* in the jejunal *Lgr5*+ cells (Figure 4A and B). Acute administration of hGly2–GLP-2 increased *Mcm3* expression in the ISCs by 122% ($P < .05$), whereas levels of the other cell-cycle transcripts was not altered in these cells (Figure 4C and D).

To establish the requirement for GLP-2R signaling in the ISC S-phase induction by GLP-2, *Lgr5*-eGFP-IRES-creERT2 mice were treated with GLP-2³⁻³³, at a dose established to antagonize the GLP-2R in vivo in mice,¹² 3.5 hours before being killed (Figure 5A). GLP-2³⁻³³ reduced the proportion of eGFP+EdU+ cells by 27% ($P < .05$) (Figure 5B) without affecting the total number of ISCs per crypt (Figure 5C). A

similar trend was noted in the proportion of OLFM4+EdU+ ISCs (decreased by 18%; $P = .051$) (Figure 5D and E). Furthermore, acute GLP-2R blockade using GLP-2³⁻³³ decreased jejunal mucosal expression of *Mcm3*, *Mcm5*, *Mcm7*, *Cdk2*, *Ccnd1*, and *s100a6* ($P < .05$) (Figure 6). Collectively, gain- and loss-of-function experiments using acute GLP-2 and GLP-2³⁻³³ administration, respectively, suggest that GLP-2 stimulates *Lgr5*+ ISC proliferation through the induction of G1/S-phase licensing.

Intriguingly, changes in acute S-phase gene expression were found to align with directional trends in the expression of *Igf1*, a known downstream mediator of the proliferative actions of GLP-2,^{19,35} increasing with hGly2–GLP-2 (Figure 3) and decreasing with GLP-2³⁻³³ ($P < .05$) treatment (Figure 6). Therefore, to evaluate whether acute changes in ISC S-phase progression with GLP-2 treatment were maintained chronically, and whether they are mediated through downstream IGF-1R signaling, we examined GLP-2 action using Intestinal epithelial (IE)-IGF-1R knockout (KO) mice (Figure 7A). In control mice, chronic treatment with hGly2–GLP-2 increased the total number of OLFM4+ cells per crypt (by 15%; $P < .05$), indicative of ISC expansion, while maintaining the percentage of these cells that were in S-phase (Figure 7B). The stimulatory effect of hGly2–GLP-2 on ISC cell number was lost in the IE-IGF-1R KO mice, although, again, overall ISC proliferation levels were not affected (Figure 7C). These results suggest that chronic GLP-2 treatment causes ISC population expansion, resulting in an increased total number of proliferating ISCs, in an IE-IGF-1R-dependent manner.

Discussion

Proliferation of the intestinal *Lgr5*+/*Olfm4*+ ISCs is essential for homeostatic maintenance of the intestinal epithelium, and is regulated by well-defined signals secreted by niche cells surrounding the crypt.¹⁻⁴ Teduglutide is a Food and Drug Administration–approved therapeutic for short-bowel syndrome that stimulates intestinal proliferation and increases mucosal growth and nutrient absorption in both human beings and rodents.²⁴⁻²⁶ Although GLP-2 stimulates proliferation of the transit-amplifying cells in the crypt,^{19,20,27,28} whether GLP-2 also enhances proliferation of the *Lgr5*+/*Olfm4*+ ISCs has not been determined. The results of the present study show that GLP-2 acutely induces S-phase cell-cycle progression in the ISCs through the GLP-2R, and stimulates ISC expansion chronically in an IGF-1R–dependent fashion.

Acute hGly2–GLP-2 treatment at $t = -6$ and -3 hours increased the proportion of both the *Lgr5*-eGFP+ and the

Figure 2. (See previous page). Acute hGly2–GLP-2 treatment induces entry of jejunal *Lgr5*+ ISCs into S-phase. (A) Representative images of *Lgr5*+ ISCs in early and late S-phase, as determined by the full and speckled nuclear distribution of EdU, respectively, using higher magnification of the images shown in Figure 1. (B) Percentage of eGFP+EdU+ ISCs in early vs late S-phase. (C) Acute pulse-chase protocol; the green mouse indicates use of *Lgr5*-eGFP-IRES-creERT2 animals (created using Biorender.com). (D–G) Percentage of eGFP+ ISCs (D) not in S-phase (BrdU-EdU-), (E) entering S-phase (BrdU-EdU+), (F) remaining in S-phase (BrdU+EdU+), and (G) exiting S-phase (BrdU+EdU-). (H) Representative images of the 4 different GFP+ cell types, as indicated by the white arrows: (a) BrdU-/EdU- (cells not in S-phase), (b) BrdU-/EdU+ (cells entering S-phase), (c) BrdU+/EdU+ (cells that remained in S-phase), and (d) BrdU+/EdU- (cells that exited S-phase). (B and D–G) $N = 4-6$. * $P < .05$, ** $P < .01$, and *** $P < .001$. DAPI, 4',6-diamidino-2-phenylindole.

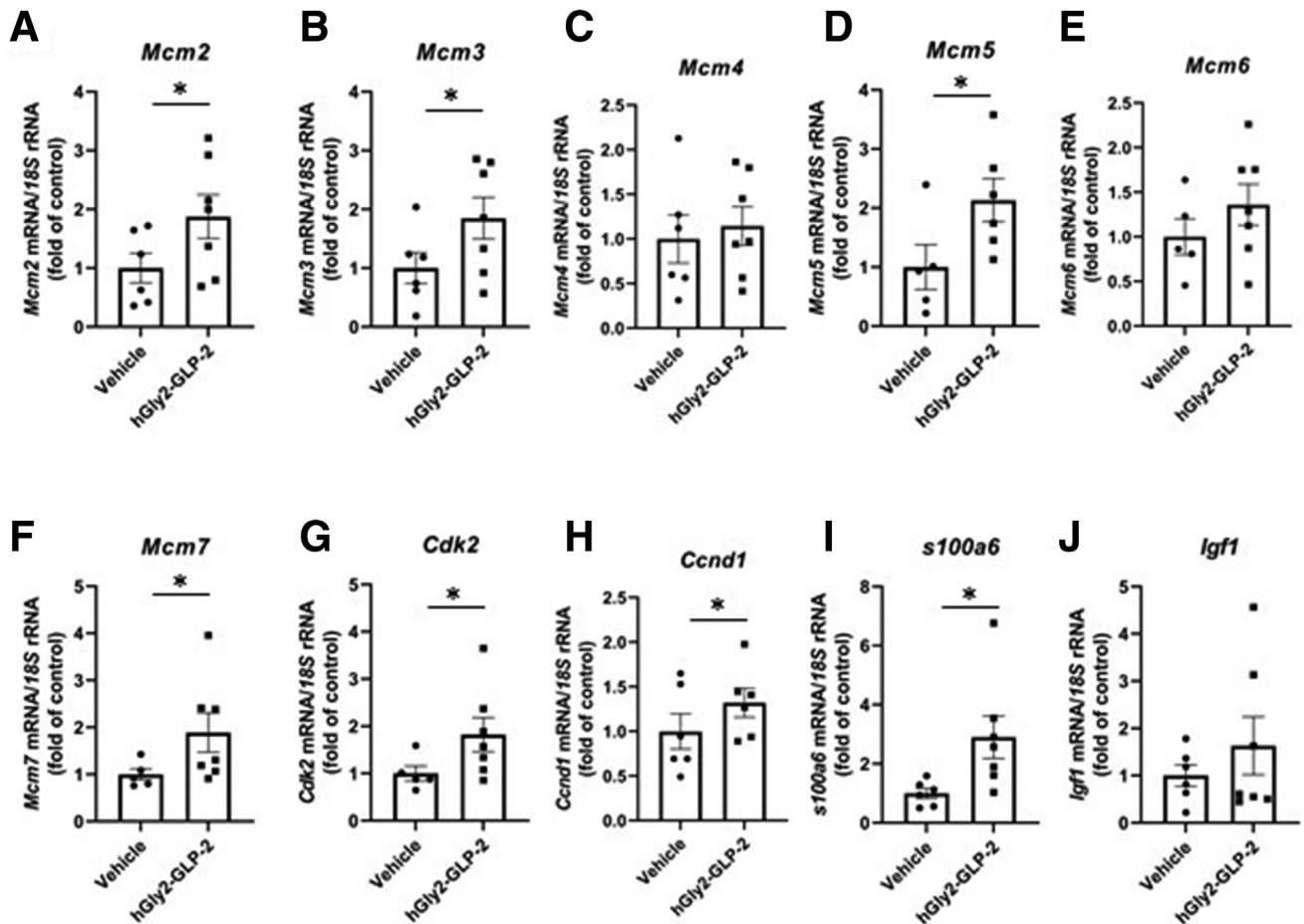


Figure 3. Acute hGly2-GLP-2 treatment increases the expression of transcripts involved in G1/S-phase transition. Jejunal mucosal isolates from the mice described in Figure 1 were analyzed by reverse-transcription quantitative polymerase chain reaction for the expression of the following: (A) *Mcm2*, (B) *Mcm3*, (C) *Mcm4*, (D) *Mcm5*, (E) *Mcm6*, (F) *Mcm7*, (G) *Cdk2*, (H) *Ccnd1*, (I) *s100a6*, and (J) *Igf1*. N = 6–7 for all panels. * $P < .05$. mRNA, messenger RNA; rRNA, ribosomal RNA.

Olfm4+ ISCs in S-phase, with the effects on the eGFP+ cells being confirmed as requiring the canonical GLP-2R. These changes occurred through induction of S-phase entry and in association with GLP-2R-dependent stimulation of several transcripts required for G1/S-phase transition, including *Mcm2*, *Mcm3*, 5, and 7, as well as of *Ccnd1*, which is required for passage through the G1/S-phase checkpoint, and *Cdk2* and *s100a6*, which are important regulators of S-phase entry.^{6,7,40,41} Notably, acute hGly2-GLP-2 treatment was found to increase the expression of *Mcm3*, but not that of several other cell-cycle markers, specifically in the *Lgr5*+ cells at the crypt base. Whether other proliferative crypt cells that are known to be stimulated by GLP-2, such as those in the TA zone,^{19,20,27,28} led to the changes in the other cell-cycle markers in the whole-thickness jejunum and/or jejunal mucosal scrapes remains to be established, as does determination of any GLP-2-regulated effects on other cell-cycle stages in the ISCs.

A recent study using MCM2 as a model for the entire MCM family of DNA helicases showed that most ISCs reside in an unlicensed G1-state, and that MCM2 binding to their DNA licenses the ISCs to pass through the G1/S cell-cycle

checkpoint and enter S-phase.⁶ It was postulated that this process creates a temporal window for proliferative fate decisions to be made in the ISCs. Using organoid cultures, it was further shown that this cell-cycle progression can be blocked by inhibition of either Wnt or epidermal growth factor (EGF) receptor (ErbB1) signaling,⁶ both of which are known to be involved in the actions of GLP-2 on intestinal crypt cells.^{19–22} When taken with the results of the present study, these findings therefore suggest that short-term GLP-2 treatment enables G1 licensing in *Lgr5*+ ISCs, thereby increasing the number of ISCs that enter the S-phase of the cell cycle.

Consistent with the findings of the present study, it has been previously reported in normal mice that approximately 25%–30% of the ISCs reside in S-phase, 10%–20% in M-phase, and 90% in G1/S/G2/M-phase, as marked by EdU/BrdU, pH3, and Ki67, respectively.^{6,42,43} However, acute administration of hGly2-GLP-2 did not affect the proportion of ISCs that were in phases of the cell cycle other than S-phase. Although Ki67 staining does detect ISCs in S-phase, it seems likely that the changes in this smaller population of cells are diluted-out by the larger percentage of total ISCs

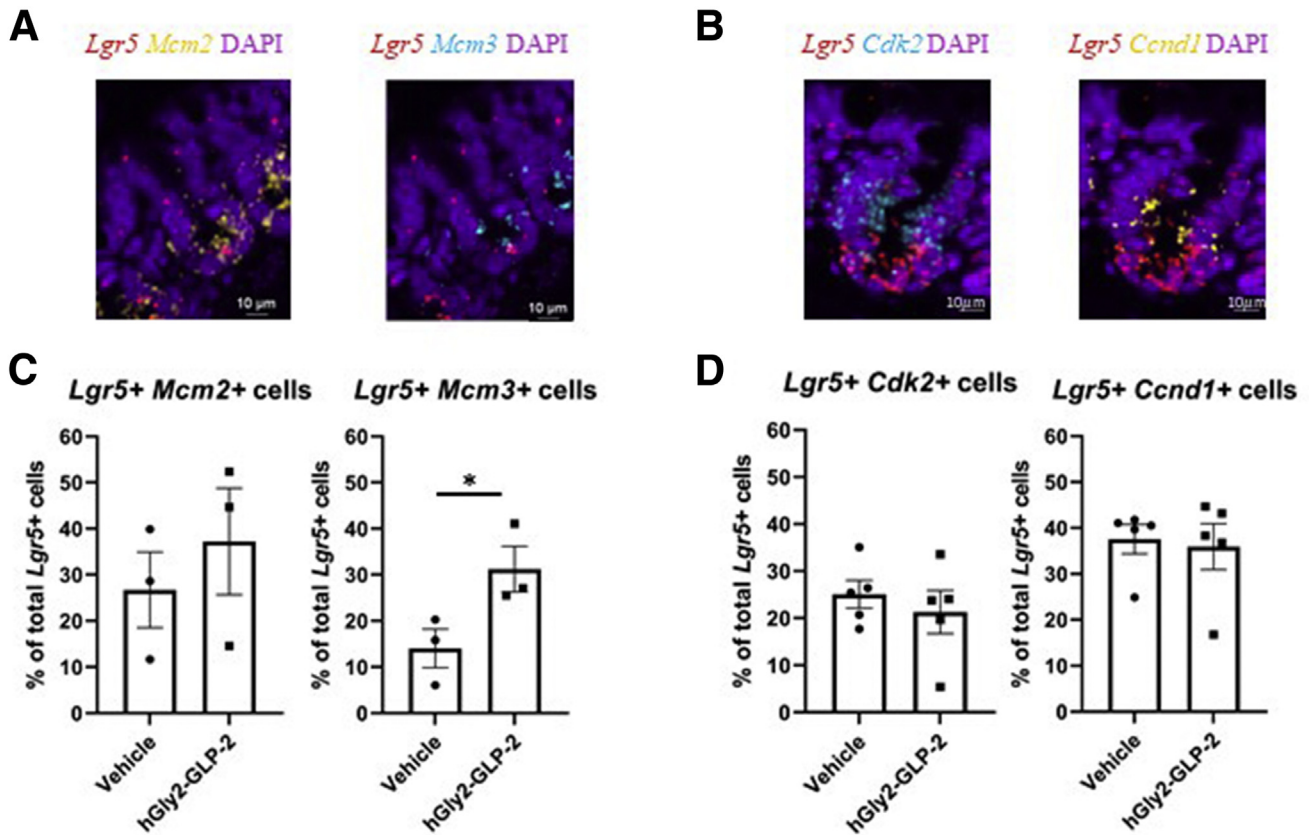


Figure 4. Acute hGly2-GLP-2 treatment increases the expression of *Mcm3* in *Lgr5*-expressing ISCs. Jejunal sections from the mice described in Figure 1 were analyzed by RNAscope for the expression of the following: (A) *Mcm2* and *Mcm3* with *Lgr5* or (B) *Cdk2* and *Ccnd1* with *Lgr5* (representative images shown). Co-expression of the following: (C) *Mcm2* and *Mcm3* with *Lgr5* and (D) *Cdk2* and *Ccnd1* with *Lgr5* was determined by quantification of the percentage of overlapping fluorescent signals in the bottom 3 cells of the crypt. (C and D) N = 3–5. * $P < .05$. DAPI, 4',6-diamidino-2-phenylindole.

expressing Ki67. Furthermore, the lack of effect of GLP-2 on other stages of the cell cycle was consistent with the findings that the number of ISCs per crypt did not change after either hGly2-GLP-2 or GLP-2³⁻³³ administration. However, *Lgr5*+ ISCs have a cell cycle of approximately 24 hours,² and it therefore is likely that progression through the entire cell cycle cannot be observed in the 3.5- to 6-hour windows used in the present study, particularly when taken with the even shorter durations of the EdU and BrdU exposure (0.5–2 h).

In contrast to our findings with acute hGly2-GLP-2 administration, chronic treatment of the IE-IGF-1R control mice did not affect the proportion of ISCs that were proliferating, but did increase the total number of ISCs per crypt, consistent with an overall enhancement of the total number of ISCs that were proliferating. A number of studies have shown that several niche-derived factors can induce ISC expansion, including not only Wnt ligands and R-spondin-1, but also IGF-1 and the ErbB ligand, neuroregulin-1.^{8,33,34,44} IGF-1R and ErbB signaling have both been identified as downstream mediators of the acute actions of GLP-2 on the intestinal epithelium,^{19–22} and the *Lgr5*+ ISCs are known to express the receptors for both IGF-1 and ErbB ligands.^{31,32} Furthermore, chronic GLP-2-stimulated growth of the

intestinal epithelial layer, as assessed by increased length of the crypt-villus axis, is impaired in mice lacking either the intestinal epithelial IGF-1R or ErbB1, and is prevented by administration of a pan-ErbB inhibitor.^{20,21,27} Hence, the chronic effects of GLP-2 to expand the ISC population in normal mice may be mediated by IGF-1R and/or ErbB signaling. Indeed, hGly2-GLP-2-induced stimulation of ISC expansion was not observed in mice that lacked the IE-IGF-1R, although the KO mice showed a normal number of ISCs per crypt. Although the ErbB1 ligand EGF is well established to regulate ISC proliferation, and is an essential component of the growth media for intestinal organoids, we recently showed that IGF-1 can restore organoid proliferation after chronic EGF withdrawal.⁴⁵ Consistent with the present findings, the small intestine of IE-IGF-1R KO mice shows normal growth parameters under basal conditions, but they do not respond appropriately to chronic administration of GLP-2, with abrogation of GLP-2-stimulated crypt cell proliferation and blunting of the growth of the crypt-villus axis.²⁷ Taken together, these findings suggest that IE-IGF-1R signaling is essential for the chronic stimulatory effects of GLP-2 on the ISCs.

Finally, the number of crypt cells expressing the *Lgr5*-eGFP transgene was found to differ quantitatively

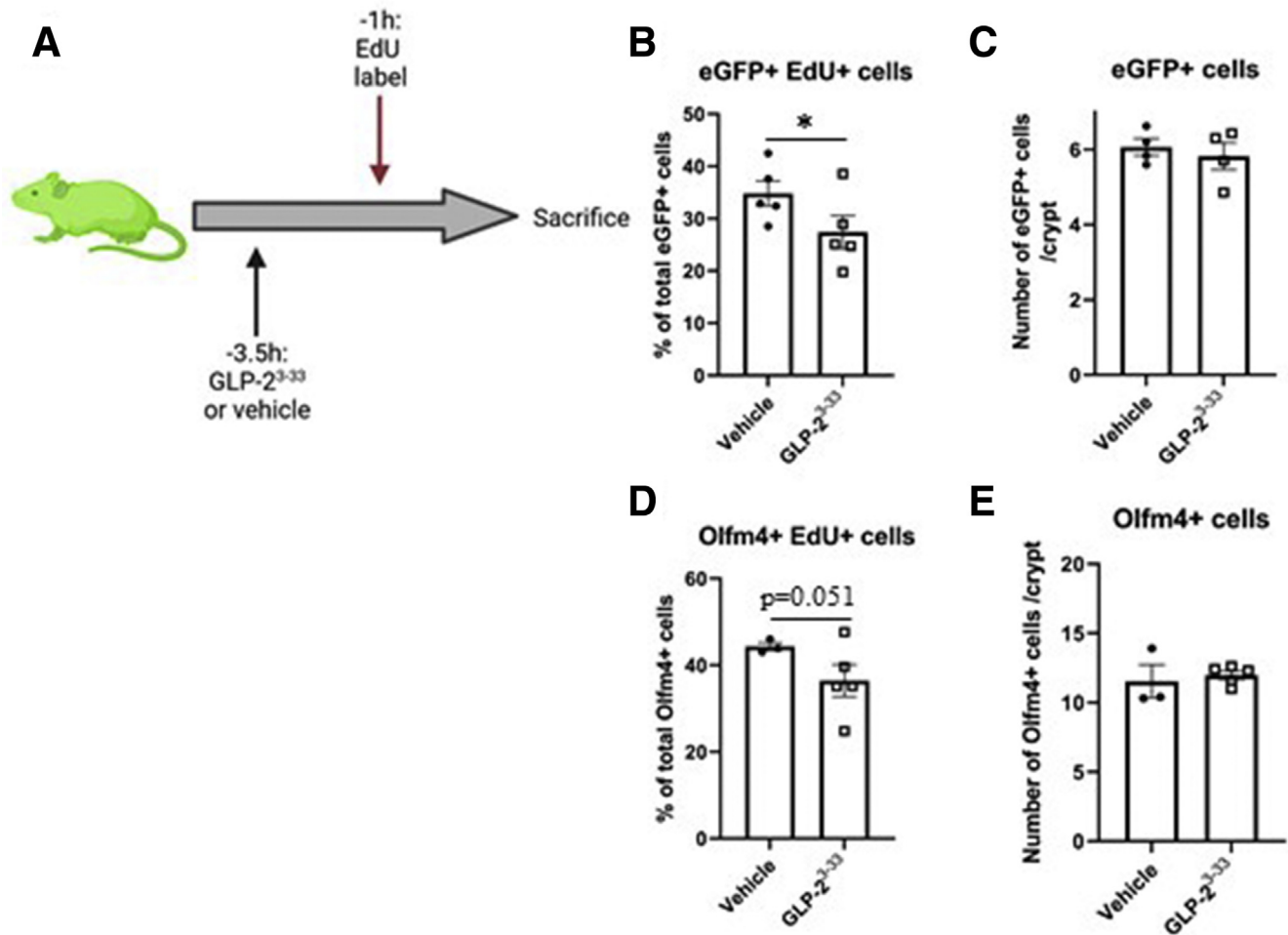


Figure 5. Acute GLP-2R antagonism decreases the proportion of jejunal *Lgr5* + ISCs in S-phase. (A) Acute GLP-2³⁻³³ treatment protocol; the *green mouse* indicates use of *Lgr5*-eGFP-IRES-creERT2 animals (created using Biorender.com). (B) Percentage of total eGFP+ ISCs that incorporated EdU. (C) Total number of eGFP+ ISCs per crypt. (D) Percentage of total OLFM4+ ISCs that incorporated EdU. (E) Total number of OLFM4+ ISCs per crypt. (B–E) N = 3–5. *P < .05.

from those that expressed the endogenous marker, *Olfm4*, under control conditions (27% vs 39%, respectively). Although both markers have been shown to be reliable for identification of the ISCs,^{2,3,5} they do differ in several regards. First, eGFP labels not only the ISCs, termed the eGFP^{high} cell population in cell sorting, but also the reserve stem cell, or the eGFP^{low} cell population.⁴⁶ A recent study using *Lgr5*-eGFP-IRES-creERT2 mice showed that eGFP immunopositivity also is detectable in ISC progenitor cells.¹¹ Furthermore, the *Lgr5*-eGFP-IRES-creERT2 mouse line shows variegated eGFP expression in the crypts owing to epigenetic silencing,⁵ whereas *Olfm4* labels ISCs in every crypt,⁵ with both patterns being observed in the present study (data not shown). Second, it has been shown through single-molecule fluorescent in situ hybridization that *Olfm4* messenger RNA is expressed in cells that are higher up in the crypt than those expressing *Lgr5*, with *Olfm4* found in border stem cells as well as the ISCs, and *Lgr5* expression restricted to ISCs in the crypt base.³ Altogether, therefore, it is not surprising that these 2 stem cell markers showed different proportions under the homeostatic conditions of

the present study. Regardless, acute administration of hGly2-GLP-2 increased the proportion of proliferating ISCs expressing both of these markers, confirming the ability of GLP-2 to stimulate ISC proliferation.

There were several limitations of the present study. First, the acute studies were restricted to a very narrow, 3.5- to 6-hour window, possibly limiting the magnitude of the responses as well as precluding determination of the effects of GLP-2 on the entire cell cycle, although this latter limitation was partially addressed in the chronic study. In addition, the possibility of a role for ErbB signaling downstream was not investigated, largely owing to the large number of ligands and receptors that are members of this family, many of which have been implicated in downstream GLP-2R signaling. Furthermore, studies on GLP-2R null mice, in addition to the current studies using the GLP-2R antagonist, would provide additional support for a role of the GLP-2R in the actions of GLP-2 on ISCs. Finally, it would be interesting to conduct more mechanistic studies on the *Lgr5*+ ISCs, perhaps using an intestinal explant model. Nonetheless, the results of the present study add GLP-2 and

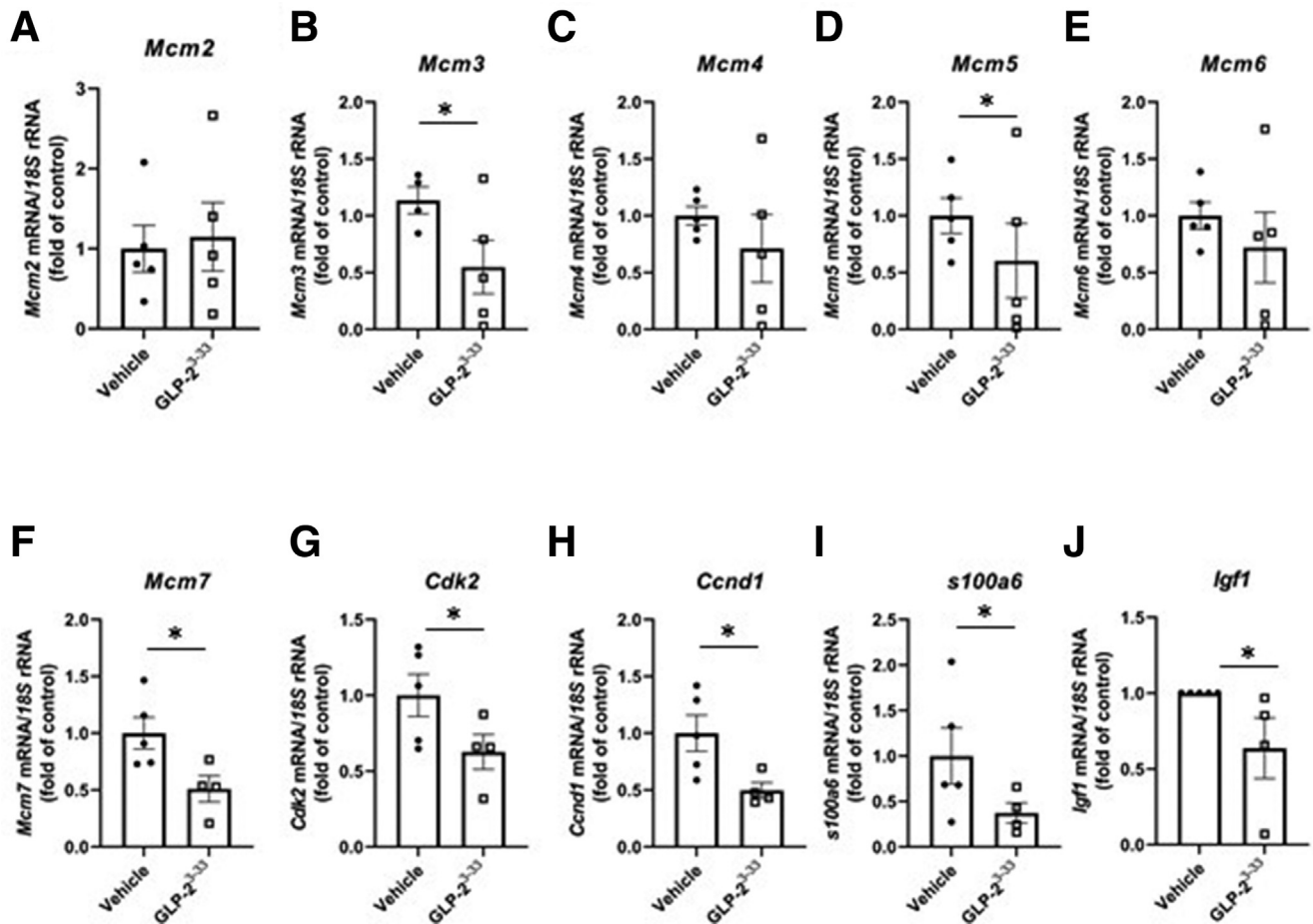


Figure 6. Acute GLP-2³⁻³³ treatment decreases the expression of transcripts involved in G1/S-phase transition. Jejunal mucosal isolates from the mice described in Figure 5 were analyzed by reverse-transcription quantitative polymerase chain reaction for the expression of the following: (A) *Mcm2*, (B) *Mcm3*, (C) *Mcm4*, (D) *Mcm5*, (E) *Mcm6*, (F) *Mcm7*, (G) *Cdk2*, (H) *Ccnd1*, (I) *s100a6*, and (J) *Igf1*. N = 5 for all panels. *P < .05. mRNA, messenger RNA; rRNA, ribosomal RNA.

its downstream signaling pathways to the growing list of niche signals that regulate the homeostatic behavior of the Lgr5+/Olfm4+ intestinal stem cell. These findings also enhance our understanding of the mechanism of action of GLP-2-based therapy to enhance intestinal growth in patients with short-bowel syndrome.

Significance

The Lgr5+ ISCs support the epithelial layer in the crypt and modulate their proliferation in response to niche signaling. The intestinal hormone GLP-2 induces gut epithelial proliferation, and a degradation-resistant GLP-2 analog, teduglutide, is used clinically to treat people with short-bowel syndrome. However, it currently is unknown whether GLP-2 modulates ISC cell behavior or number. We now show in mice that GLP-2 acutely stimulates ISC cell-cycle progression into S-phase in a GLP-2R-dependent fashion, and chronically increases ISC expansion through a pathway requiring IGF-1R signaling. These findings contribute to our understanding of the factors regulating ISC behavior as well as the beneficial effects of GLP-2-based therapy in short-bowel syndrome.

Materials and Methods

Animals

Female heterozygous Lgr5-eGFP-IRES-creERT2 mice² and male wild-type siblings were obtained from the Jackson Laboratory (Bar Harbor, ME). Animals were bred and housed under a 12-hour light/dark cycle in an animal facility at the University of Toronto. In all experiments, 6- to 14-week-old heterozygous Lgr5-eGFP-IRES-creERT2 mice were sex- and litter-matched, with both males and females used in all studies; all animals were studied in the fed state.

Female CD1 mice (from Charles River Canada [St. Constant, QC Canada] or Taconic [Taconic Biosciences, Germantown, NY]) were used at 11 weeks of age after acclimation to the facility for 8–9 days, as reported in a previous study.²⁰ Animals were studied in the fed state, and all protocols were approved by the Animal Care Committees of the University Health Network and Mount Sinai Hospital.

The IE-IGF-1R KO and control mice were reported in a previous study.⁴⁵ In brief, IE-IGF-1R KO mice were generated by crossing villin-creERT2 with *Igf1r*^{fl/fl} mice and treated with an intraperitoneal injection of 10 mg/mL tamoxifen for 5 days. Control mice included villin-

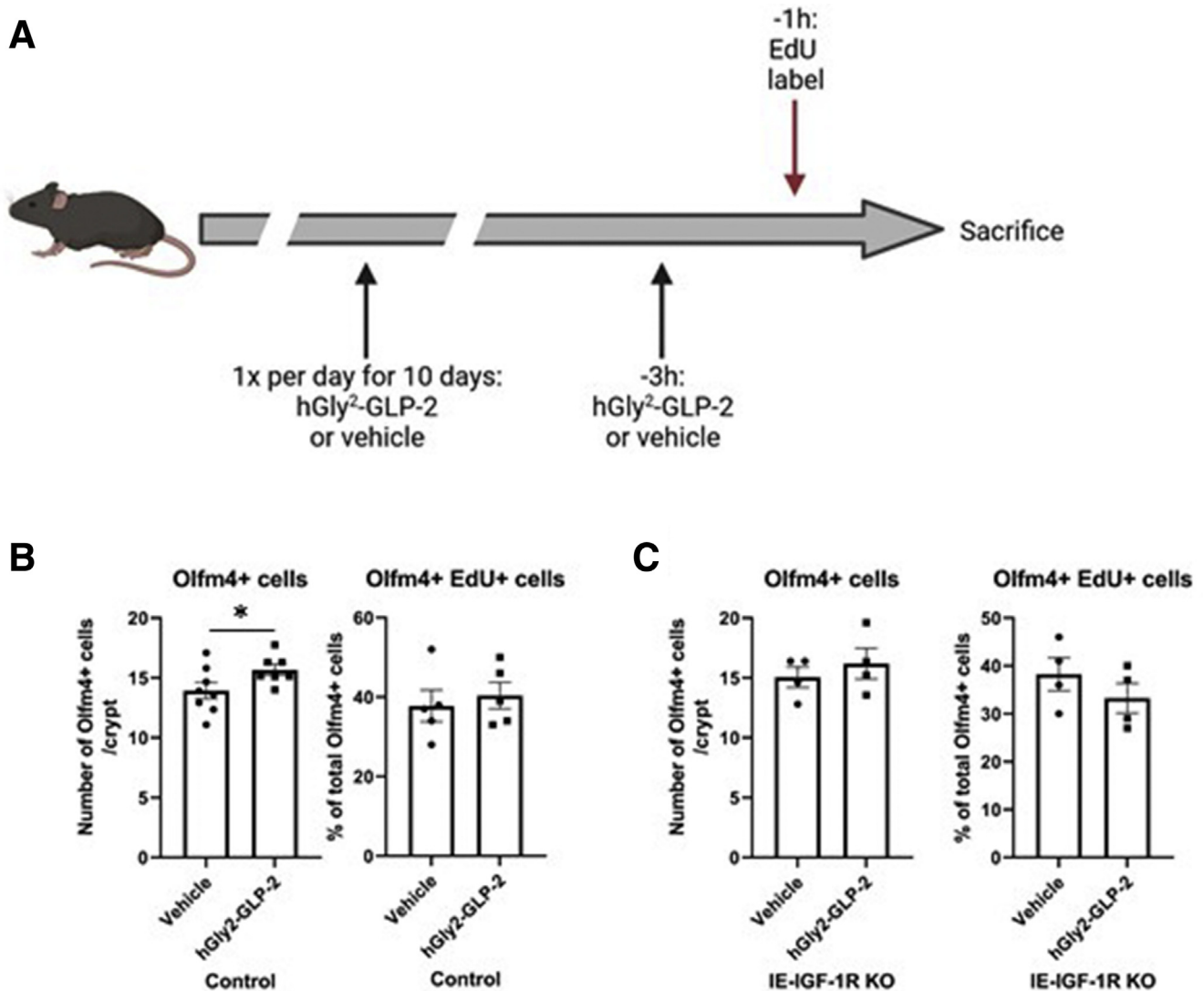


Figure 7. Chronic hGly2-GLP-2 treatment induces jejunal Lgr5+ ISC expansion. (A) Chronic hGly2-GLP-2 treatment protocol (created using Biorender.com). (B) Number of Olfm4+ ISCs per crypt (left) and the percentage of Olfm4+ ISCs that incorporated EdU (right) in control mice. (C) Number of Olfm4+ ISCs per crypt (left) and the percentage of Olfm4+ ISCs that incorporated EdU (right) in IE-IGF-1R KO mice. (B and C) N = 4-8. * $P < .05$.

creERT2 and $Igf1r^{fl/fl}$ mice treated with tamoxifen or vehicle, and villin-creERT2; $Igf1r^{fl/fl}$ mice treated with vehicle. All mice were 6-8 weeks old, and sex- and litter-matched; fed male and female mice were included in all groups.

The Animal Care Committee approved all animal experimental protocols in this study. Experimental protocol schematics were created using Biorender.com (Toronto, Canada).

Experimental Protocols

Lgr5-eGFP-IRES-creERT2 mice were treated with hGly2-GLP-2 (0.2 mg/kg body weight; American Peptide Company, Sunnyvale, CA) or phosphate-buffered saline (pH 7.4, vehicle) subcutaneously 6 and 3 hours before being killed, or with 30 ng human GLP-2³⁻³³ or vehicle intraperitoneally 3.5 hours before being killed. As previously reported, GLP-2³⁻³³ is a partial agonist of the GLP-2R.^{12,47}

Hence, at very high concentrations, GLP-2³⁻³³ can partially activate GLP-2R signaling. However, the dose of GLP-2³⁻³³ used herein (30 ng) has been fully validated as an antagonist of GLP-2 actions in vivo in mice, without exerting any agonistic activity.¹² Mice then received an intraperitoneal injection of either 2.5 mg/25 g EdU (ThermoFisher Scientific) 1 hour before being killed, or 1 mg/25 g BrdU (ThermoFisher Scientific, Mississauga, Canada) at 2 hours before being killed and 0.2 mg/25 g EdU at 0.5 hours before being killed.^{12,19,27,28,45}

CD1 mice were administered hGly2-GLP-2 (2.5 μ g, subcutaneously; Pepceutical, Ltd, Enderby, Leicestershire, UK) or vehicle, and killed after 1, 4, 8, 12, or 25 hours, as previously reported.²⁰

As previously reported,⁴⁵ IE-IGF-1R KO and control mice were treated with hGly2-GLP-2 (0.2 mg/kg body weight) or vehicle subcutaneously once a day for 10 days, with a final injection 3 hours before being killed on day 11. All mice

Table 1. Primary and Secondary Antibodies Used in Immunofluorescent Staining of Formalin-Fixed and Paraffin-Embedded Jejunal Cross-Sections

Primary antibody	Primary antibody source, product number, and RRID	Dilution	Secondary Alexa Fluor conjugated antibody	Secondary antibody source, product number, and RRID	Nikon swept field confocal laser line
Rabbit anti-GFP	Invitrogen, A11122, AB_221569	1:100	Goat anti-rabbit IgG Alexa Fluor 488	ThermoFisher Scientific, A-11008, AB_143165	488 nm
Mouse anti-pH3	Cell Signaling (Whitby, Canada), 9706S, RRID not available	1:400	Goat anti-mouse IgG Alexa Fluor 555	ThermoFisher Scientific, A-21422, AB_2535844	561 nm
Rat anti-Ki67	Invitrogen, 14-5698-82, AB_10854564	1:200	Goat anti-rat IgG Alexa Fluor 555	ThermoFisher Scientific, A-21434, AB_2535855	561 nm
Rabbit anti-OLFM4	Cell Signaling, 39141S, RRID not available	1:200	Goat anti-rabbit IgG Alexa Fluor 488	ThermoFisher Scientific, A-11008, AB_143165	488 nm
Rat anti-BrdU	Abcam (Waltham, MA), ab6326, RRID not available	1:200	Goat anti-rat IgG Alexa Fluor 647	ThermoFisher Scientific, A-21247, AB_141778	604 nm

RRID, Research Resource Identifier.

received an intraperitoneal injection of 2.5 mg/25 g EdU 1 hour before being killed.

Mice were killed and the small intestine was isolated and flushed with phosphate-buffered saline. Two-centimeter sections of jejunum and colon were flash-frozen and stored at -80°C or were fixed in 10% buffered formalin for paraffin-embedding and sectioning (University Health Network Histological Services, Toronto, Canada).

Immunofluorescent Staining and Quantification

Formalin-fixed, paraffin-embedded jejunal cross-sections were immunostained for GFP, pH3, Ki67, BrdU, and/or OLFM4, using the primary and secondary antisera listed in Table 1. The Click-iT EdU Alexa Fluor 488 Imaging Kit (Invitrogen, Toronto, Canada) was used for detection of EdU. Stained sections were incubated with 4',6-diamidino-2-phenylindole (ThermoFisher Scientific), mounted with SlowFade Gold Antifade Mountant (ThermoFisher Scientific), and imaged using a Zeiss Axioplan 2 Imaging Microscope (Toronto, Canada) or a Nikon Swept Field Confocal microscope with NIS-Elements Imaging software (Nikon Corporation, Mississauga, Canada). Co-localization of eGFP with EdU, pH3, Ki67, or EdU/BrdU, as well as of OLFM4 with EdU, was counted in 100–635 eGFP+ or OLFM4+ cells per mouse to make N = 1. The number of eGFP+ or OLFM4+ cells per well-oriented crypt was quantified in a minimum of 8 crypts per mouse to make N = 1. Identification of GFP+ cells in early S-phase vs late S-phase, by the appearance of full or speckled EdU nuclear staining, respectively,^{6,39} was determined in 31–118 eGFP+EdU+ cells per mouse to make N = 1. All staining, imaging, and quantification was performed in a blinded manner.

Gene Expression Analyses

For microarray analysis, RNA was extracted from full-thickness sections of jejunum and colon using TRIzol (ThermoFisher Scientific, Mississauga, Canada), and pooled samples were analyzed by Affymetrix (chip MG_U74Av2 for

jejunum, and MG_U74Av2 for colon, ThermoFisher Scientific, Mississauga, Canada). To identify differentially expressed genes, data were normalized with the Affymetrix Microarray Analysis Suite 5.0 software and using the Robust Multichip Average (Microarray Analysis Suite)⁴⁸; log ratios were compared.

RNA was extracted from jejunal mucosal scrapes using the RNeasy Plus Mini Kit with QiaShedder (Qiagen, Inc, Toronto, Canada), reverse-transcribed with 5× All-In-One Reverse Transcriptase MasterMix (Applied Biological Materials, Richmond, Canada), and analyzed by quantitative polymerase chain reaction using TaqMan Fast Advanced Master Mix (ThermoFisher Scientific) with the primers listed in Table 2. Data were analyzed using the Delta delta cycle threshold method with 18S as the internal control.⁴⁹ Note that because of the large number of transcripts and replicates assayed, the samples for Igf1 from the GLP-2³⁻³³-treated mice (only) were analyzed on separate plates, with each value for GLP-2³⁻³³ being normalized to its plate-

Table 2. Quantitative Polymerase Chain Reaction TaqMan Primers (ThermoFisher Scientific, Mississauga, Canada)

Target gene	Product code (TaqMan)
<i>Mcm2</i>	Mm00484815_m1
<i>Mcm3</i>	Mm05676815_s1
<i>Mcm4</i>	Mm00725863_s1
<i>Mcm5</i>	Mm00484840_m1
<i>Mcm6</i>	Mm00484848_m1
<i>Mcm7</i>	Mm04207570_g1
<i>Cdk2</i>	Mm00443947_m1
<i>Ccnd1</i>	Mm00432359_m1
<i>s100a6</i>	Mm00771682_g1
<i>Igf1</i>	Mm00439559_m1
18S	Hs99999901_s1

specific vehicle control, resulting in a loss of variance for the data from these vehicle-treated animals (Figure 6f).

RNAscope for triplex detection of *Lgr5* with *Mcm2* and *Mcm3*, and of *Lgr5* with *Ccnd1* and *Cdk2* was conducted using the Multiplex Fluorescent Reagent Kit v2 from ACD Biotechnie (Newark, NJ) as per the manufacturer's instructions. Expression of the transcripts was counted in 15–20 crypts per mouse to make $N = 1$. Signals were counted in a blinded fashion.

Statistics

Data are presented as means \pm SEM. Statistical differences between 2 groups were determined by the Student *t* test, or by 2-way analysis of variance followed by the Student *t* test for post hoc analysis, as appropriate. GraphPad Prism (GraphPad Software, Inc, San Diego, CA) was used for statistical tests.

All authors had access to the study data and reviewed and approved the final manuscript.

References

1. Marshman E, Booth C, Potten CS. The intestinal epithelial stem cell. *Bioessays* 2002;24:91–98.
2. Barker N, van Es JH, Kuipers J, Kujala P, van den Born M, Cozijnsen M, Haegebarth A, Korving J, Begthel H, Peters PJ, Clevers H. Identification of stem cells in small intestine and colon by marker gene *Lgr5*. *Nature* 2007;449:1003–1007.
3. Munoz J, Stange DE, Schepers AG, van de Wetering M, Koo BK, Itzkovitz S, Volckmann R, Kung KS, Koster J, Radulescu S, Myant K, Versteeg R, Sansom OJ, van Es JH, Barker N, van Oudenaarden A, Mohammed S, Heck AJ, Clevers H. The *Lgr5* intestinal stem cell signature: robust expression of proposed quiescent '+4' cell markers. *EMBO J* 2012;31:3079–3091.
4. Gehart H, Clevers H. Tales from the crypt: new insights into intestinal stem cells. *Nat Rev Gastroenterol Hepatol* 2019;16:19–34.
5. Schuijers J, van der Flier LG, van Es J, Clevers H. Robust cre-mediated recombination in small intestinal stem cells utilizing the *olm4* locus. *Stem Cell Reports* 2014;3:234–241.
6. Carroll TD, Newton IP, Chen Y, Blow JJ, Nathke I. *Lgr5*(+) intestinal stem cells reside in an unlicensed G1 phase. *J Cell Biol* 2018;217:1667–1685.
7. Arata Y, Fujita M, Ohtani K, Kijima S, Kato JY. Cdk2-dependent and -independent pathways in E2F-mediated S phase induction. *J Biol Chem* 2000;275:6337–6345.
8. Van Landeghem L, Santoro MA, Mah AT, Krebs AE, Dehmer JJ, McNaughton KK, Helmrath MA, Magness ST, Lund PK. IGF1 stimulates crypt expansion via differential activation of 2 intestinal stem cell populations. *FASEB J* 2015;29:2828–2842.
9. Richmond CA, Shah MS, Deary LT, Trotter DC, Thomas H, Ambruzs DM, Jiang L, Whiles BB, Rickner HD, Montgomery RK, Tovaglieri A, Carlone DL, Breault DT. Dormant intestinal stem cells are regulated by PTEN and nutritional status. *Cell Rep* 2015;13:2403–2411.
10. Shoshkes-Carmel M, Wang YJ, Wangenstein KJ, Toth B, Kondo A, Massasa EE, Itzkovitz S, Kaestner KH. Subepithelial telocytes are an important source of Wnts that supports intestinal crypts. *Nature* 2018;557:242–246.
11. Jarde T, Chan WH, Rossello FJ, Kaur Kahlon T, Theocharous M, Kurian Arackal T, Flores T, Giraud M, Richards E, Chan E, Kerr G, Engel RM, Prasko M, Donoghue JF, Abe SI, Phesse TJ, Nefzger CM, McMurrick PJ, Powell DR, Daly RJ, Polo JM, Abud HE. Mesenchymal niche-derived neuregulin-1 drives intestinal stem cell proliferation and regeneration of damaged epithelium. *Cell Stem Cell* 2020;27:646–662 e7.
12. Shin ED, Estall JL, Izzo A, Drucker DJ, Brubaker PL. Mucosal adaptation to enteral nutrients is dependent on the physiologic actions of glucagon-like peptide-2 in mice. *Gastroenterology* 2005;128:1340–1353.
13. Iakubov R, Lauffer LM, Trivedi S, Kim Y-I, Brubaker PL. Carcinogenic effects of exogenous and endogenous glucagon-like peptide-2 in azoxymethane-treated mice. *Endocrinology* 2009;150:4033–4043.
14. Trivedi S, Wiber SC, El-Zimaity HM, Brubaker PL. Glucagon-like peptide-2 increases dysplasia in rodent models of colon cancer. *Am J Physiol Gastrointest Liver Physiol* 2011;302:G840–G849.
15. Wismann P, Barkholt P, Secher T, Vrang N, Hansen HB, Jeppesen PB, Baggio LL, Koehler JA, Drucker DJ, Sandoval DA, Jelsing J. The endogenous preproglucagon system is not essential for gut growth homeostasis in mice. *Mol Metab* 2017;6:681–692.
16. Drucker DJ, Erlich P, Asa SL, Brubaker PL. Induction of intestinal epithelial proliferation by glucagon-like peptide 2. *Proc Natl Acad Sci U S A* 1996;93:7911–7916.
17. Brubaker PL. Glucagon-like peptide-2 and the regulation of intestinal growth and function. *Compr Physiol* 2018;8:1185–1210.
18. Yusta B, Matthews D, Koehler JA, Pujadas G, Kaur KD, Drucker DJ. Localization of glucagon-like peptide-2 receptor expression in the mouse. *Endocrinology* 2019;160:1950–1963.
19. Dube PE, Forse CL, Bahrami J, Brubaker PL. The essential role of insulin-like growth factor-1 in the intestinal tropic effects of glucagon-like peptide-2 in mice. *Gastroenterology* 2006;131:589–605.
20. Yusta B, Holland D, Koehler JA, Maziarz M, Estall JL, Higgins R, Drucker DJ. ErbB signaling is required for the proliferative actions of GLP-2 in the murine gut. *Gastroenterology* 2009;137:986–996.
21. Feng Y, Demehri FR, Xiao W, Tsai YH, Jones JC, Brindley CD, Threadgill DW, Holst JJ, Hartmann B, Barrett TA, Teitelbaum DH, Dempsey PJ. Interdependency of EGF and GLP-2 signaling in attenuating mucosal atrophy in a mouse model of parenteral nutrition. *Cell Mol Gastroenterol Hepatol* 2017;3:447–468.
22. Shawe-Taylor M, Kumar JD, Holden W, Dodd S, Varga A, Giger O, Varro A, Dockray GJ. Glucagon-like peptide-2 acts on colon cancer myofibroblasts to stimulate proliferation, migration and invasion of both myofibroblasts

- and cancer cells via the IGF pathway. *Peptides* 2017; 91:49–57.
23. Drucker DJ, Shi Q, Crivici A, Sumner-Smith M, Tavares W, Hill M, DeForest L, Cooper S, Brubaker PL. Regulation of the biological activity of glucagon-like peptide 2 in vivo by dipeptidyl peptidase IV. *Nat Biotechnol* 1997;15:673–677.
 24. Jeppesen PB, Sanguinetti EL, Buchman A, Howard L, Scolapio JS, Ziegler TR, Gregory J, Tappenden KA, Holst J, Mortensen PB. Teduglutide (ALX-0600), a dipeptidyl peptidase IV resistant glucagon-like peptide 2 analogue, improves intestinal function in short bowel syndrome patients. *Gut* 2005;54:1224–1231.
 25. Jeppesen PB, Gilroy R, Pertkiewicz M, Allard JP, Messing B, O’Keefe SJ. Randomised placebo-controlled trial of teduglutide in reducing parenteral nutrition and/or intravenous fluid requirements in patients with short bowel syndrome. *Gut* 2011;60:902–914.
 26. Pevny S, Maasberg S, Rieger A, Karber M, Bluthner E, Knappe-Drzikova B, Thurmann D, Buttner J, Weylandt KH, Wiedenmann B, Muller VA, Blaker H, Pascher A, Pape UF. Experience with teduglutide treatment for short bowel syndrome in clinical practice. *Clin Nutr* 2019;38:1745–1755.
 27. Rowland KJ, Trivedi S, Wan K, Kulkarni RN, Holzenberger M, Robine S, Brubaker PL. Loss of glucagon-like peptide-2-induced proliferation following intestinal epithelial insulin-like growth factor-1 receptor deletion. *Gastroenterology* 2011; 141:2166–2175.
 28. Smither BR, Pang HY, Brubaker PL. Glucagon-like peptide-2 requires a full-complement of Bmi-1 for its proliferative effects in the murine small intestine. *Endocrinology* 2016;157:2660–2770.
 29. Bjercknes M, Cheng H. Modulation of specific intestinal epithelial progenitors by enteric neurons. *Proc Natl Acad Sci U S A* 2001;98:12497–12502.
 30. Koopmann MC, Chen X, Holst JJ, Ney DM. Sustained glucagon-like peptide-2 infusion is required for intestinal adaptation, and cessation reverses increased cellularity in rats with intestinal failure. *Am J Physiol Gastrointest Liver Physiol* 2010;299: G1222–G1230.
 31. Grun D, Lyubimova A, Kester L, Wiebrands K, Basak O, Sasaki N, Clevers H, van Oudenaarden A. Single-cell messenger RNA sequencing reveals rare intestinal cell types. *Nature* 2015;525:251–255.
 32. Yan KS, Gevaert O, Zheng GXY, Anchang B, Probert CS, Larkin KA, Davies PS, Cheng ZF, Kaddis JS, Han A, Roelf K, Calderon RI, Cynn E, Hu X, Mandleywala K, Wilhelmy J, Grimes SM, Corney DC, Boutet SC, Terry JM, Belgrader P, Ziraldo SB, Mikkelsen TS, Wang F, von Furstenberg RJ, Smith NR, Chandrakesan P, May R, Chrissy MAS, Jain R, Cartwright CA, Niland JC, Hong YK, Carrington J, Breault DT, Epstein J, Houchen CW, Lynch JP, Martin MG, Plevritis SK, Curtis C, Ji HP, Li L, Henning SJ, Wong MH, Kuo CJ. Intestinal enteroendocrine lineage cells possess homeostatic and injury-inducible stem cell activity. *Cell Stem Cell* 2017;21:78–90 e6.
 33. Basak O, Beumer J, Wiebrands K, Seno H, van Oudenaarden A, Clevers H. Induced quiescence of Lgr5+ stem cells in intestinal organoids enables differentiation of hormone-producing enteroendocrine cells. *Cell Stem Cell* 2017;20:177–190 e4.
 34. Bohin N, McGowan KP, Keeley TM, Carlson EA, Yan KS, Samuelson LC. Insulin-like growth factor-1 and mTORC1 signaling promote the intestinal regenerative response after irradiation injury. *Cell Mol Gastroenterol Hepatol* 2020;10:797–810.
 35. Dube PE, Rowland KJ, Brubaker PL. Glucagon-like peptide-2 activates beta-catenin signaling in the mouse intestinal crypt: role of insulin-like growth factor-I. *Endocrinology* 2008;149:291–301.
 36. Pereira PD, Serra-Caetano A, Cabrita M, Bekman E, Braga J, Rino J, Santus R, Filipe PL, Sousa AE, Ferreira JA. Quantification of cell cycle kinetics by EdU (5-ethynyl-2'-deoxyuridine)-coupled-fluorescence-intensity analysis. *Oncotarget* 2017;8:40514–40532.
 37. Hans F, Dimitrov S. Histone H3 phosphorylation and cell division. *Oncogene* 2001;20:3021–3027.
 38. Sun X, Kaufman PD. Ki-67: more than a proliferation marker. *Chromosoma* 2018;127:175–186.
 39. Krude T, Musahl C, Laskey RA, Knippers R. Human replication proteins hCdc21, hCdc46 and P1Mcm3 bind chromatin uniformly before S-phase and are displaced locally during DNA replication. *J Cell Sci* 1996; 109:309–318.
 40. Matsumoto T, Murao S, Kito K, Kihana T, Matsuura S, Ueda N. Modulation of S-100 genes response to growth conditions in human epithelial tumor cells. *Pathol Int* 1997;47:339–346.
 41. Fu M, Wang C, Li Z, Sakamaki T, Pestell RG. Cyclin D1: normal and abnormal functions. *Endocrinology* 2004; 145:5439–5447.
 42. Kim TH, Saadatpour A, Guo G, Saxena M, Cavazza A, Desai N, Jadhav U, Jiang L, Rivera MN, Orkin SH, Yuan GC, Shivdasani RA. Single-cell transcript profiles reveal multilineage priming in early progenitors derived from Lgr5(+) intestinal stem cells. *Cell Rep* 2016; 16:2053–2060.
 43. Sheng X, Lin Z, Lv C, Shao C, Bi X, Deng M, Xu J, Guerrero-Juarez CF, Li M, Wu X, Zhao R, Yang X, Li G, Liu X, Wang Q, Nie Q, Cui W, Gao S, Zhang H, Liu Z, Cong Y, Plikus MV, Lengner CJ, Andersen B, Ren F, Yu Z. Cycling stem cells are radioresistant and regenerate the intestine. *Cell Rep* 2020;32:107952.
 44. Yan KS, Janda CY, Chang J, Zheng GXY, Larkin KA, Luca VC, Chia LA, Mah AT, Han A, Terry JM, Ootani A, Roelf K, Lee M, Yuan J, Li X, Bolen CR, Wilhelmy J, Davies PS, Ueno H, von Furstenberg RJ, Belgrader P, Ziraldo SB, Ordonez H, Henning SJ, Wong MH, Snyder MP, Weissman IL, Hsueh AJ, Mikkelsen TS, Garcia KC, Kuo CJ. Non-equivalence of Wnt and R-spondin ligands during Lgr5(+) intestinal stem-cell self-renewal. *Nature* 2017;545:238–242.
 45. Fesler Z, Mitova E, Brubaker PL. GLP-2, EGF, and the intestinal epithelial IGF-1 receptor interactions in the regulation of crypt cell proliferation. *Endocrinology* 2020; 161:bqaa040.

46. Barker N. Adult intestinal stem cells: critical drivers of epithelial homeostasis and regeneration. *Nat Rev Mol Cell Biol* 2014;15:19–33.
47. Thulesen J, Knudsen LB, Hartmann B, Hastrup S, Kissow H, Jeppesen PB, Orskov C, Holst JJ, Poulsen SS. The truncated metabolite GLP-2 (3-33) interacts with the GLP-2 receptor as a partial agonist. *Regul Peptide* 2002;103:9–15.
48. Irizarry RA, Hobbs B, Collin F, Beazer-Barclay YD, Antonellis KJ, Scherf U, Speed TP. Exploration, normalization, and summaries of high density oligonucleotide array probe level data. *Biostatistics* 2003;4:249–264.
49. Livak KJ, Schmittgen TD. Analysis of relative gene expression data using real-time quantitative PCR and the 2(-delta delta C(T)) method. *Methods* 2001; 25:402–408.

CRediT Authorship Contributions

Maegan E. Chen (Data curation: Lead; Formal analysis: Lead; Investigation: Lead; Methodology: Lead; Writing – original draft: Lead)

Setareh Malekian Naeini (Data curation: Supporting; Investigation: Supporting; Writing – review & editing: Supporting)

Arjuna Srikrishnaraj (Investigation: Supporting; Writing – review & editing: Supporting)

Daniel J. Drucker (Conceptualization: Lead; Data curation: Supporting; Funding acquisition: Lead; Investigation: Supporting; Methodology: Equal; Writing – review & editing: Supporting)

Zivit Fesler (Data curation: Lead; Investigation: Lead; Writing – review & editing: Supporting)

Patricia L. Brubaker, PhD (Conceptualization: Lead; Funding acquisition: Lead; Investigation: Supporting; Methodology: Equal; Project administration: Lead; Resources: Lead; Supervision: Lead; Writing – review & editing: Equal)

Conflicts of interest

These authors disclose the following: Patricia L. Brubaker is a consultant to ProLynx, Novome, VectivBio AG, and Zealand Pharma; and Daniel J. Drucker has served as a consultant or speaker within the past 12 months to Eli Lilly, Inc, Forkhead Biotherapeutics, Kallyope, Merck Research Laboratories, Novo Nordisk, Inc, and Pfizer, Inc. GLP-2 is the subject of a patent license agreement between Takeda Inc. and the University of Toronto, Toronto General Hospital (University Health Network). The remaining authors disclose no conflicts.

Funding

This work was supported by Canadian Institutes of Health Research operating grants PJT-14853 (P.L.B.) and 154321 (D.J.D.). Some of the equipment was supported by the 3D (Diet, Digestive Tract and Disease) Centre funded by the Canadian Foundation for Innovation and Ontario Research Fund (project numbers 19442 and 30961). Also supported by a Canadian Institutes of Health Research Frederick Banting and Charles Best Canada Graduate Scholarship and an Ontario Graduate Scholarship (M.E.C.); by a summer studentship from the Canadian Association of Gastroenterology (S.M.N.); by a Banting and Best Diabetes Centre Novo Nordisk Chair and a Novo Nordisk Foundation Sinai Health Fund in Regulatory Peptides (D.J.D.), and by a Tier 1 Canada Research Chair in Vascular and Metabolic Biology (P.L.B.).

Received September 13, 2021. Accepted February 14, 2022.

Correspondence

Address correspondence to: Patricia L. Brubaker, PhD, Medical Sciences Building, Room 3366, University of Toronto, 1 King's College Circle, Toronto, Ontario M5S 1A8, Canada. e-mail: p.brubaker@utoronto.ca; fax: 1 (416) 978-4940.

Acknowledgments

The authors are extremely grateful to Drs B. Yusta (University of Toronto, Toronto, Ontario, Canada) and M. Maziarz (currently at Lund University Diabetes Center, Malmö, Sweden) for the generation and analysis of the microarray data, and Mr D. Tsang (University of Toronto, Toronto, Ontario, Canada) for assistance with the RNAscope methodology.